Acquirement of Rituximab Resistance in Lymphoma Cell Lines Is Associated with Both Global *CD20* Gene and Protein Down-Regulation Regulated at the Pretranscriptional and Posttranscriptional Levels

Myron S. Czuczman,[1,2] Scott Olejniczak,[2] Aruna Gowda,[2] Adam Kotowski,[2] Arvinder Binder,[1] Harman Kaur,[1] Joy Knight,[2] Petr Starostik,[3] Julie Deans,[4] and Francisco J. Hernandez-Ilizaliturri[1,2]

Abstract Acquirement of resistance to rituximab has been observed in lymphoma patients. To define mechanisms associated with rituximab resistance, we developed various rituximab-resistant cell lines (RRCL) and studied changes in CD20 expression/structure, lipid raft domain (LRD) reorganization, calcium mobilization, antibody-dependent cellular cytotoxicity, and complement-mediated cytotoxicity (CMC) between parental and RRCL. Significant changes in surface CD20 antigen expression were shown in RRCL. Decreased calcium mobilization and redistribution of CD20 into LRD were found in RRCL. Western blotting identified a unique 35 kDa protein band in RRCL, which was not seen in parental cells and was secondary to an increase in surface and cytoplasmic expression of IgM light chains. *CD20* gene expression was decreased in RRCL. *In vitro* exposure to PS341 increased CD20 expression in RRCL and minimally improved the sensitivity to rituximab-associated CMC. Our data strongly suggest that the acquisition of rituximab resistance is associated with global gene and protein down-regulation of the CD20 antigen affecting LRD organization and downstream signaling. CD20 expression seems to be regulated at the pretranscriptional and posttranscriptional levels. Proteasome inhibition partially reversed rituximab resistance, suggesting the existence of additional mediators of rituximab resistance. Future research is geared to identify drugs and/or biological agents that are effective against RRCL.

Rituximab is an IgGκ chimeric monoclonal antibody (mAb) directed against the CD20 antigen expressed on normal B cells and the majority of mature B-cell neoplasms (1). Several biological effects have been attributed to rituximab antitumor activity, including antibody-dependent cellular cytotoxicity (ADCC), complement-mediated cytotoxicity (CMC), and induction of apoptosis/antiproliferation (2–13). Evidence strongly supports that ADCC mediated by cytotoxic lymphocytes, monocyte/macrophages, and neutrophils may be the predominant *in vivo* mechanism of action of rituximab (12, 13).

Binding of rituximab to surface CD20 on B-cell lymphoma cells results in the activation of the Src family of protein tyrosine kinases, leading to phosphorylation of PLCγ2 and increased cytoplasmic Ca^{2+} (3–11). These early signal transduction events activate caspase-3 to promote B-cell apoptosis (11). Reorganization of the CD20 receptor into LRD is observed following rituximab exposure and precedes the aforementioned signaling events (14, 15). Structural changes in CD20 likely affect its redistribution within the LRD and decrease the cellular responses to rituximab (15).

It is postulated that the majority of patients retreated with rituximab will eventually relapse with variable degrees of resistant disease (16). There is an urgent need to conduct translational studies that will explore the mechanisms of resistance to mAbs in non–Hodgkin's lymphoma (NHL), and to develop therapeutic strategies to limit and/or overcome resistance pathways.

Therapeutic strategies combining rituximab with systemic chemotherapy result in higher response rates and an improvement in survival (17, 18). An alternative strategy by which to potentially minimize treatment-related toxicities, while maximizing rituximab activity, is by using an extended rituximab induction schedule and/or maintenance program(s). "Repeated exposure" of NHL cells to rituximab could lead to an increasing incidence of clinical rituximab resistance. The effect of rituximab resistance with respect to tumor responsiveness to subsequent biological or chemotherapy treatment in lymphoma patients is currently unknown.

Mechanisms for tumor resistance to mAb therapy that have been postulated can be divided into tumor-related [e.g., down-regulation of targeted extracellular CD20 antigen, acquisition

Authors' Affiliations: Departments of [1]Medicine, [2]Immunology, and [3]Molecular Diagnostics, Roswell Park Cancer Institute, Buffalo, New York and [4]University of Calgary, Calgary, Alberta, Canada

Received 5/21/07; revised 9/18/07; accepted 11/14/07.

Grant support: Research in part, supported as a sub-project on NIH PO1 grant CA103985-1 Awarded to the Garden State Cancer Center, Belleville, NJ.

The costs of publication of this article were defrayed in part by the payment of page charges. This article must therefore be hereby marked *advertisement* in accordance with 18 U.S.C. Section 1734 solely to indicate this fact.

Conflict of interest disclosure: The authors declare no competing financial interests.

Requests for reprints: Myron S. Czuczman, Lymphoma/Myeloma Service, Roswell Park Cancer Institute, Elm and Carlton Streets, Buffalo, NY 14263. Phone: 716-845-3221; E-mail: myron.czuczman@roswellpark.org.

doi:10.1158/1078-0432.CCR-07-1254

of a protective phenotype (by up-regulation of complement inhibitory proteins, etc.)] or host-related factors (e.g., Fcγ receptor polymorphisms; refs. 19–26). Complete CD20 expression loss has been reported in anecdotal case reports involving a small number of patients (20). One of the major limitations in defining the mechanisms of resistance to rituximab is the lack of a laboratory model by which unlimited supplies of "resistant" cells may be repeatedly and extensively studied over an extended period of time. Using a rituximab-resistant model, we show that on the development of rituximab resistance, significant changes occur to the CD20 antigen, including (*a*) a moderate down-regulation of CD20; (*b*) altered reorganization of CD20 into the LRD; and (*c*) a possible role for the ubiquitin-proteasome system in the degradation of the COOH-terminal of CD20. In addition, we show increased expression of complement inhibitory proteins (CD55, CD59) as well as unexpected up-regulation of surface and cytoplasmic IgM and CD52.

Materials and Methods

Cell lines and generation of rituximab-resistant cell lines. The studies were conducted in several rituximab-sensitive (RSCL) and rituximab-resistant (RRCL) cell lines. Raji and RL cells were purchased from the American Type Culture Collection. The Raji cell lines are well-characterized Burkitt's lymphoma cell lines. The RL cell line is an EBV-negative diffuse large B-cell lymphoma cell line. The SU-DHL-4 cell line, which is a transformed follicular lymphoma cell line, was a kind gift of Dr. Steven Treon (Dana-Farber Cancer Institute, Boston, MA). The cells were maintained in RPMI 1640 supplemented with HEPES 5 mmol/L, sodium pyruvate 1 mmol/L, penicillin and streptomycin (100 IU/mL), and 10% heat-inactivated fetal bovine serum (RPMI-10).

RRCL were generated from Raji, SU-DHL4, and RL cells (Table 1). For the development of resistant cell lines, sensitive parental cell lines were maintained in RPMI-10 and once the log phase of growth was reached, the cells were divided into two groups. In the first group, cells were incubated at 37°C, 5% CO_2 and serially exposed for 24 h to an escalating dose of rituximab (0.1-128 μg/mL). The second group of lymphoma cells was exposed for 24 h to an escalating dose of rituximab (same dose range as in group 1) plus an escalating concentration of human serum (dilution 1:1,000 up to 1:1.875) as a source of complement. Following the 24 h incubation with rituximab ± human serum, cells were centrifuged and the medium was replaced with fresh RPMI 1640-10. Cells were then allowed to regrow for a minimum of 3 days, and once exponential log phase of growth was reached, the procedure was repeated for a total of 10 passages at which time functional assays (i.e., ADCC, CMC) showed maximal inhibition of rituximab-associated biological activity.

Antibodies. Rituximab (Biogen Idec and Genentech) was obtained from the RPCI Pharmacy Department. The testing dose of anti-CD20 used for the present studies was 10 μg/mL. Chimeric anti-human Her-2neu (trastuzumab) was used as an isotype.

For phenotypic analysis, purified phycoerythrin-conjugated monoclonal mouse anti-human CD80 and CD45RO as well as FITC-conjugated mouse anti-human CD45RA and a PC-conjugated mouse anti-human CD19 were obtained from Beckman Coulter, Inc. FITC-conjugated mouse anti-human CD20, HLA-DR, and CD40; and phycoerythrin-conjugated mouse anti-human CD59 as well as Cy-Chrome–conjugated mouse anti-human CD55 mAbs were purchased from BD PharMingen, Inc. A tricolor mouse anti-human CD22 and an allophycocyanin-labeled mouse anti-human CD52 were obtained from Caltag Laboratories. Finally, FITC-goat anti-mouse and phycoerythrin-goat anti-human mAbs were used as isotype controls (BD PharMingen). An allophycocyanin-conjugated mouse anti-human anti-CD79a (BD PharMingen) was used to detect changes in surface IgM.

For Western blot studies, two polyclonal rabbit anti-human antibodies were used to detect the internal domain of CD20 antigen as previously described (15, 27). The antibody 1439 recognizes the NH_2-terminal region whereas the antibody GST-77 binds specifically to the COOH-terminal region of the intracellular domain of CD20. Two polyclonal rabbit anti-human anti-ubiquitin–activating enzyme (E1) and anti-human ubiquitin conjugating enzyme (E2) were obtained from Calbiochem Laboratories. Appropriate secondary antibodies were obtained from Stressgen Biotechnology.

Functional assays to asses rituximab-mediated ADCC and CMC. To show a decrease in biological activity in the RRCL, we did standard ^{51}Cr release assays to asses rituximab-mediated CMC and ADCC. For CMC assays, 5×10^6 NHL cell lines (i.e., RSCL and RRCL) were labeled for 2 h at 37°C with 3.7 MBq of ^{51}Cr (100 μCi). The radioactive excess was washed out thrice in PBS and the tumor cells were resuspended at a final concentration of 1×10^6/mL on RPMI-10 medium.

From the initial tumor cell suspension, 100 μL aliquots (1×10^5 cells per well) were placed in 96-well plates. Subsequently, NHL cells were preincubated with RPMI-10, rituximab, or isotype control (10 μg/mL) in combination with human serum (dilution 1:4). Pooled human serum collected from healthy donors was used as a source of complement. Serum samples were obtained under protocol CIC 01-16, approved by Roswell Park Cancer Institute Institutional Review Board. Subsequently, cells were incubated at 37°C, 5% CO_2 for 6 h. A separate set of ^{51}Cr-labeled NHL cells (1×10^5 per well) were incubated in RPMI-10 and treated with 50 μL of a 1% Triton solution to determine maximum chromium release. Finally, the 96-well plates were centrifuged at 1,400 rpm (300 × *g*), 4°C for 5 min and the supernatant of each well was collected individually and γ emission was measured by the Packard Auto-Gamma Cobra II series counting system (IBM, Inc.).

ADCC assays were done using peripheral blood mononuclear cells at an effector to target ratio of 40:1 for 6 h as previously described (28).

The percentage of specific ^{51}Cr release (lysis) was calculated using the standard formula: %lysis = [(test sample release - background release) / (maximum release - background release)] × 100. All samples were run in triplicate in three different sets of experiments. Results are reported as a mean values with SE.

In vivo resistance to rituximab was evaluated and clearly shown using Raji-4RH in a lymphoma-bearing xenograft mouse model (Supplementary Fig. 1).

Table 1. Nomenclature describing RRCL and clones generated from three B-cell NHL cell lines (Raji, RL, and SU-DHL-4)

Cell type	Parental cell	Resistant cell	Resistant cell
Exposure	None Raji; SU-DHL-4; RL	Rituximab alone 2R; DHL4-2R; RL-2R	Rituximab + human serum 4RH; DHL4-4RH; RL-4RH

NOTE: Resistance to rituximab was obtained under two different selective pressures, rituximab alone or rituximab in combination with pooled human serum as a complement source.

Table 2. cDNA microarrays done using the Roswell Park Cancer Institute Cancer Chip showed several genetic changes (primarily up-regulation) in the ubiquitin-proteasome system among the rituximab-resistant cell lines, 2R and 4RH, when compared with rituximab-sensitive parental Raji cell line

Specific genes	2R	4RH
	Up-regulated (log exp) compared with Raji parental cells	Up-regulated (log exp) compared with Raji parental cells
Ubiquitin system		
Ubiquitin-activating enzyme (E1)	+2.32	+2.61
Ubiquitin-conjugating enzyme (E2)	+2.33	+3.36
Ubiquitin thiolesterase	+2.29	+3.02
Proteasome system		
Proteasome subunit β type 5	+2.17	+2.15
Proteasome 26S	+3.18	+4.08

NOTE: Values of +2.0 or greater are statistically significant.

Calcium (Ca^{2+}) mobilization following* in vitro *exposure to rituximab in RSCL and RRCL. Ca^{2+} mobilization was measured by flow cytometric analysis using FLUO-3 AM (acetoxymethyl ester, Molecular Probes/Invitrogen, Inc.). Pluronic acid F-127 (Molecular Probes/Invitrogen) was used to load FLUO-3 AM into NHL cells. Optimization of the Ca^{2+} indicator and calibration curves was done for each cell line using the Ca^{2+} calibration kit from Molecular Probes. Raji and RRCL were labeled under optimal conditions with FLUO-3 AM/Pluronic Acid F-127. Subsequently, cells were then resuspended in Hanks' medium with Ca^{2+} and exposed to rituximab or isotype (10 μg/mL) with or without human serum (25%). Raji cells exposed to ionomycin were used as positive controls. Fluorescence excitation was measured at 525 nm. Experiments were done in triplicates. Ca^{2+} concentration was calculated using the following formula: nanomolar $[Ca^{2+}] = K_d$ (i.e., effective dissociation constant for calcium-bound FLUO-3) × [(fluorescence of the sample - fluorescence of the probe in the absence of Ca^{2+}) / (fluorescence of the positive control - fluorescence of the sample)].

Differences in rituximab binding between RSCL and RRCL. To evaluate whether the decrease in rituximab-associated biological activity in our cell lines was a result of a decrease in the binding affinity of rituximab for CD20, we did flow cytometric studies using an Alexa-conjugated rituximab produced in the flow cytometry facilities at Roswell Park Cancer Institute.

Evaluation of changes in CD20 antigen and immunoglobulin expression in RRCL. Differences in CD20 antigen expression and density of expression between RSCL and RRCL were evaluated by flow cytometric analysis. In addition, structural changes in CD20 were evaluated by Western blotting. RSCL and RRCL (5×10^6 cells) were solubilized with a radioimmunoprecipitation assay buffer containing 2 mmol/L phenylmethylsulfonyl fluoride, leupeptin (1 μg/mL), pepstatin (1 μg/mL), and aproprotinin (1 μg/mL). After nuclei and debris were pelleted, the total protein was quantified. Subsequently, 20 to 30 μg of protein per fraction were resolved under reducing or nonreducing conditions on a 10% SDS-PAGE gel and separated. The gel was then electroblotted (24 V × 16 h) onto a polyvinylidene difluoride membrane (Schleicher and Schuell). After blocking, membranes were incubated at 4°C overnight with various antibodies that target different epitopes on the internal (1439 and GST-77 antibodies) and external (rituximab) CD20 domains. After adding the appropriate horseradish peroxidase–conjugated secondary antibody, detection by enhanced chemiluminescence methods were done.

Differences in CD20 transcription in RRCL. Studies were conducted in Raji parental cells and RRCL 2R and 4RH derived from Raji cells. Total RNA was extracted from RSCL and RRCL using TRIzol reagent and used as templates for the creation of cDNA using random primers. CD20 was specifically amplified from cDNA using primers designed to amplify its coding region (sense, ATGGGACTTTCCCGCAG; antisense, ATCACTTAAGGAGAGCTGTC). Thirty cycles of PCR were done and PCR products were electrophoresed through 1% agarose gels containing ethidium bromide. Resultant bands visualized on a BioDoc-It System UV transluminator (UVP).

CD20 *gene sequencing.* The *CD20* gene is composed of eight exons giving rise to mRNA splice variants of 2.6, 2.8 (dominant), and 3.4 kb. To explain differences in the structure of CD20 (see Results) observed between RSCL and RRCL, we did gene sequencing of CD20 using cells derived from parental Raji cells and two RRCL. Total RNA was isolated from cell lines with TRIzol (Sigma; ref. 29). RNA was then reverse transcribed into cDNA using random hexamers and Moloney murine leukemia virus reverse transcriptase and the CD20 coding sequence (~1 kb) amplified by PCR with primers specific for the 5′ and 3′ ends of the coding region. The product was run on a 1% agarose gel, specific bands were excised, and DNA was purified using a commercially available kit (Qiagen). Purified CD20 cDNA was then ligated into the pGEM-T Easy vector (Promega). This vector was used to transform DH5α chemically competent *Escherichia coli* (Invitrogen) and these cells were grown overnight in the presence of ampicillin. Transformed cells were then selected based on isopropyl-L-thio-β-D-galactopyranoside/Xgal blue/white selection and further expanded in 3 mL of Luria-Bertani medium containing ampicillin. Plasmid DNA was extracted from *E. coli* via standard alkaline lysis miniprep (29) and tested for CD20 insertion by restriction digest. Plasmid DNA was sent to the Roswell Park Cancer Institute Biopolymer Facility for sequencing from the T7 and/or SP6 promoters contained within pGEM. Sequencing was done directly, with the ABI Big Dye Terminator kit (Applied Biosystems); the reaction products were resolved on automated capillary sequencer, ABI 3100, and evaluated using the DNA Sequencing Analysis software version 3.7. The sequence was compared with the CD20 wild-type sequence deposited at Locus Link.

RNA splicing differences between RRCL and RSCL as determined by Northern blot. To further study the potential mechanisms responsible for the changes in CD20 observed in RRCL, we explored the role, if any, of alternative splicing in changes observed on CD20 expression in RRCL. Total RNA was extracted from RSCL (Raji) and RRCL (2R and 4RH) using TRIzol reagent as described above. Total RNA was then heated to 55°C for 15 min followed by electrophoresis through a 1.4% agarose gel containing 18% formaldehyde. Following electrophoresis, RNA was transferred to nitrocellulose membranes as previously described (30, 31). RNA was then UV cross-linked to membranes and probed with ^{32}P-labeled cDNA specific for CD20 or β-actin. Probes used were an ~870 bp cDNA encompassing the coding region of CD20 and an ~600 bp β-actin cDNA, which were labeled to a specific activity of 1×10^9 dpm/mg. Autoradiographic detection of a hybridized probe

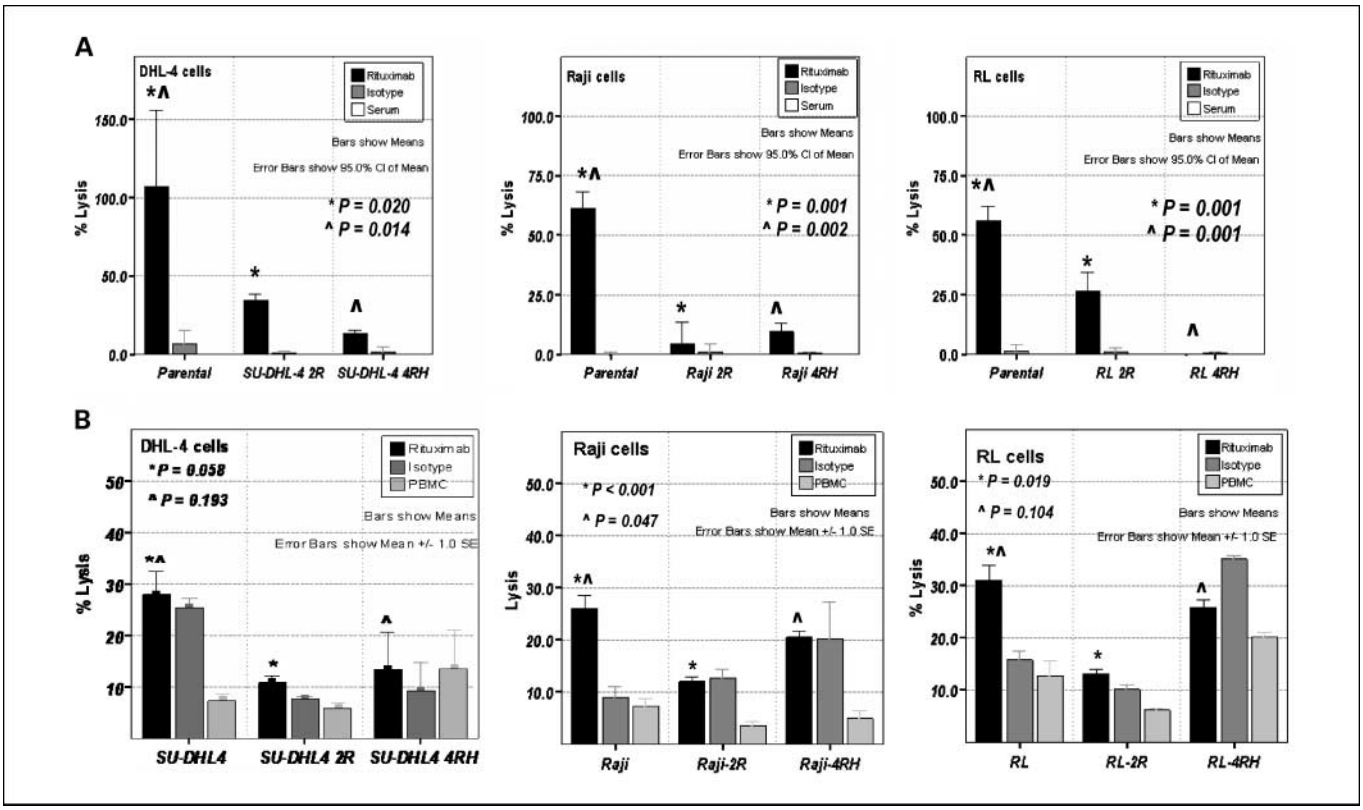

Fig. 1. Rituximab-resistant cells derived from DHL-4, Raji, and RL cells have significant impairment to rituximab-induced CMC (*A*) or ADCC (*B*) as determined by ^{51}Cr release assays. ^{51}Cr-labeled NHL cells were exposed to rituximab or isotype (10 mg/mL) and human serum or peripheral blood mononuclear cells (*PBMC*) at an effector-to-target ratio of 40:1, respectively. ^{51}Cr release was measured and the percentage of lysis was calculated.

was done along with phosphoimaging using a Molecular Dynamics STORM scanner.

Genetic changes associated with the acquisition of resistance to rituximab. To elucidate possible changes in gene expression profiles that may be associated with potential pathways involved in the development of rituximab resistance, we conducted experiments comparing rituximab-sensitive Raji cells with the two RRCL derived from it (2R and 4RH) applying cDNA microarray technology. Total RNA was extracted from each cell line and cDNA was generated as previously described (32). Labeled cDNA was hybridized to the Roswell Park Cancer Institute Cancer Chip, containing 11,519 cDNAs and subsequently scanned to obtain quantitative gene expression levels. Data were analyzed by the Genomic Core Facilities in the Department of Genetics, RPCI.

[^{35}S]methionine labeling. To study if changes in CD20 expression observed between RSCL and RRCL were the result of an increase in protein degradation, we conducted [^{35}S]methionine labeling studies in Raji cells. Rituximab-sensitive or rituximab-resistant cells (1×10^7) were removed from a log-phase growth culture and resuspended at 1×10^7 cells/mL in methionine-free DMEM (Life Technologies) for 30 min at 37°C. After the 30-min incubation, 0.7 mCi/mL of [^{35}S] methionine (Amersham) was added and cells were incubated at 37°C for 2.5 h. Subsequently, 1-mL aliquots were removed and added to 10 mL of ice-cold 1× PBS. Cells were then pelleted by centrifugation for 5 min at 1,400 rpm, supernatant was removed, and the cell pellet was lysed in a 1% Triton X-100 buffer containing protease and phosphatase inhibitors. Immunoprecipitation was then carried out using rituximab (CD20) or trastuzumab (Her2/neu; negative control) at a concentration of 2 μg/mL. Eluted proteins were then separated on 12% SDS-PAGE gels and detected by autoradiography.

Evaluation of differences in CD20 antigen redistribution into lipid raft domains following rituximab exposure between RSCL and RRCL. NHL cells were grown to a density of 1×10^6/mL to 3×10^6/mL in RPMI 1640-10 medium as described above; 1×10^8 cells were harvested by centrifugation at 2,000 rpm for 5 min in a Sorvall Legend RT Centrifuge. The supernatant was discarded and the cells were gently resuspended in 10 mL of RPMI 1640-10 medium. Raji cells (1×10^8) were suspended in 10 mL of RPMI – 10% fetal bovine serum and exposed to rituximab or trastuzumab (isotype) at a final concentration of 10 μg/mL for 15 min at 37°C, 5%CO_2. Lipid rafts were isolated as described by Cheng et al. (33). CD20 and Lyn localization in soluble and insoluble fractions were determined by Western blotting as previously described (36).

Effects of proteasome inhibition with PS341 on the expression of the CD20 in RRCL. Raji-derived 2R cells (4×10^6) were exposed to PS341 (Millennium Pharmaceuticals, Inc.) at 0, 20, and 100 nmol/L. After 24 or 48 h, proteins were extracted, revolted in a 13% SDS gel, and transferred into polyvinylidene difluoride membranes. CD20 expression was detected with the GST-77 (COOH terminal), 1439 (NH_2-terminal), and rituximab antibodies.

Results

Chronic exposure to rituximab with or without human serum results in acquirement of a resistant phenotype to rituximab-induced ADCC and CMC. Significant reduction in rituximab-mediated CMC and ADCC was observed in RRCL. Acquirement of a resistant phenotype was shown in cells derived from Raji, RL, and SU-DHL-4 cell lines (Table 1; Figs. 1 and 2). Rituximab resistance had been maintained in our RRCL over the past 2 years despite multiple passages or prolonged periods of incubation. Moreover, rituximab resistance has been preserved without the necessity to supplement rituximab into the

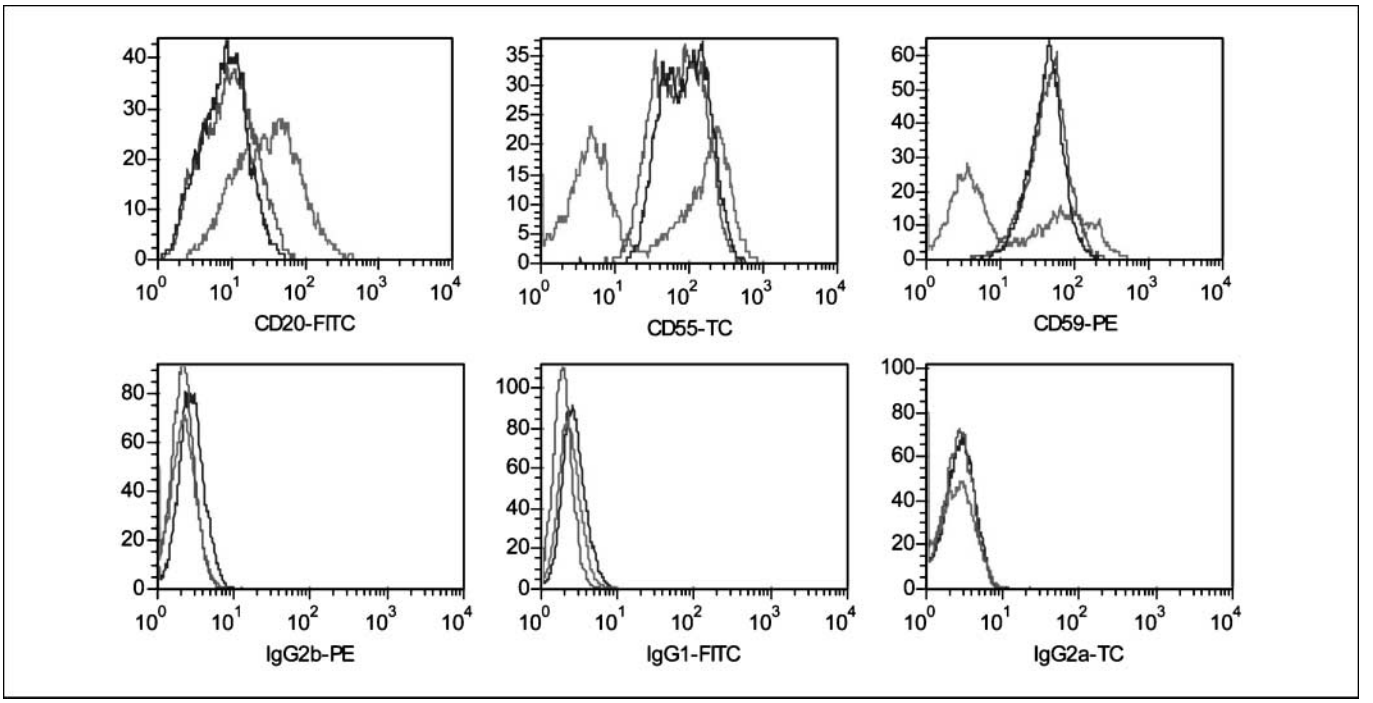

Fig. 2. Acquirement of rituximab resistance resulted in up-regulation of the complement inhibitory proteins CD55 and to a lesser degree CD59 as determined by multicolor flow cytometric analysis. In addition, up-regulation of CD52 was found to be present in RRCL Raji-2R (*blue line*) and Raji-4RH (*green line*) derived from Raji cells (*red line*). Similar findings were observed in cell lines derived from RL and SU-DHL4 cells (not shown). Modest changes (i.e., down-regulation) in surface CD20 and no changes in CD19, CD22, CD80, and class II antigens were observed across RRCL when compared with their respective parental cells.

medium in which the cells grow in between experiments. *In vivo* rituximab resistance was confirmed with Raji-4RH cells (see Supplementary Fig. 1).

Phenotypic changes occurring in rituximab resistant cell lines. Repeated exposure of rituximab-sensitive cells to rituximab with or without human serum resulted in significant changes in the surface expression of various cluster-designated antigens. Specifically, an up-regulation of the complement inhibitory proteins CD55 and CD59, as well as CD52, was observed (Fig. 2). In contrast, no significant changes in the expression of CD22, CD19, CD80, and class II antigens CD46 and CD40 were shown (not shown). Overall, global down-regulation of

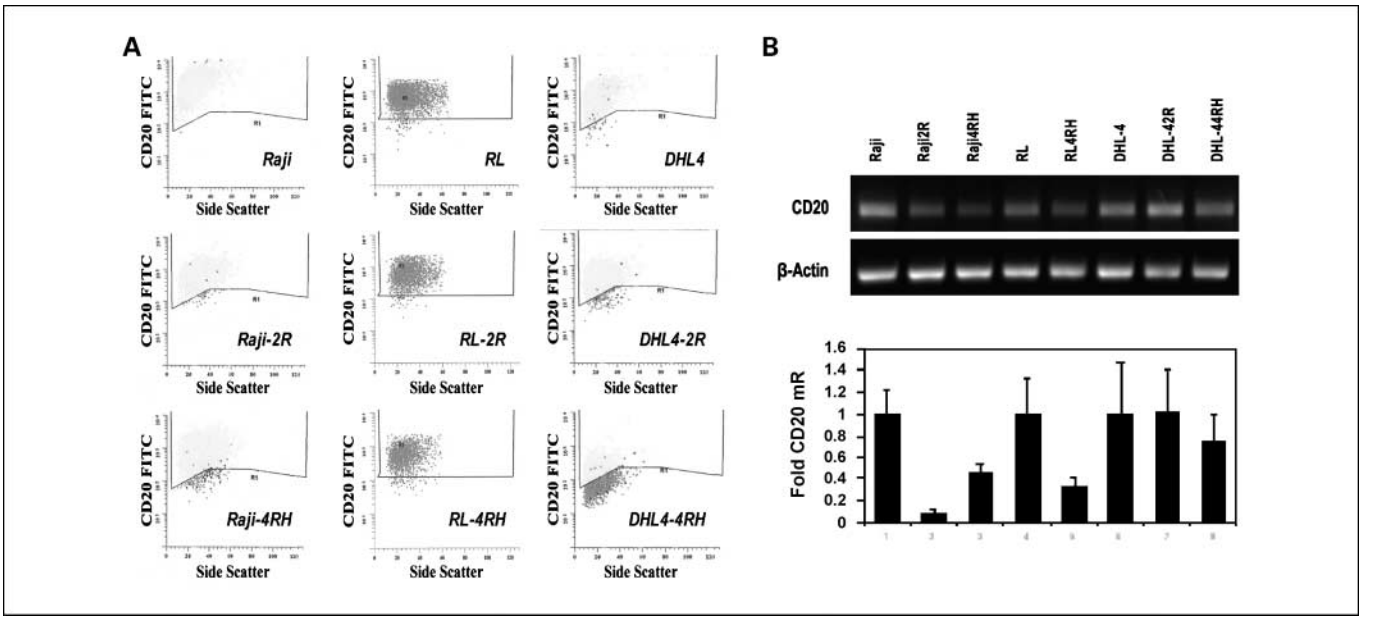

Fig. 3. A decrease in CD20 expression was noted by flow cytometric analysis between rituximab-sensitive and rituximab-resistant cells. Flow cytometry shows a decrease in CD20 expression in RRCL (*A*). In general, reverse transcription-PCR using primers encompassing the coding region of CD20 shows decreased CD20 transcription in RRCL compared with rituximab-sensitive cell lines Raji, SU-DHL4, and RL cells (*B*).

CD20 was shown in all RRCL (Figs. 3 and 4A). Of interest, only in Burkitt's-derived cells, a down-regulation of CD21 was observed upon the acquirement of a rituximab-resistant phenotype (data not shown).

Development of rituximab resistance is associated with significant changes in CD20 antigen expression. The repeated exposure of lymphoma cells to rituximab with or without human serum led to a decrease in CD20 expression between rituximab-sensitive (Raji, 186.3 MFC) cells and RRCL (2R, 167.76 MFC and 4RH, 151 MFC) as shown by flow cytometric studies using rituximab. Similar differences were observed in RRCL derived from RL and SU-DHL-4 cells (Fig. 3A). This decrease in surface CD20 levels can be attributed, in part, to reduced CD20 transcription in the resistant lines (Fig. 3B). Western blot analysis using rituximab shows that full-length CD20 is diminished in the resistant lines compared with Raji (compare band migrating at 40 kDa in Fig. 4, *top*). Strikingly, a novel lower molecular weight species (30 kDa) appears in the resistant lines 2R and 4RH that is not apparent in the parental Raji line. Studies done in nonreducing conditions failed to show the existence of a postulated truncated form of CD20, but instead the lower molecular weight species observed at 30 kDa was subsequently identified as the light chain of IgM (see below).

Development of rituximab resistance is associated with up-regulation of surface IgM. Western blot analysis using rituximab and a horseradish peroxidase–conjugated anti-human secondary mAb shows that full-length CD20 is down-regulated in RRCL compared with potential Raji cells from which they were derived (Fig. 4A). Strikingly, a novel lower molecular weight species (~30 kDa) was detected in resistant 2R and 4RH cell lines but not in parental Raji or RL (not shown) cell lines. We have recently discovered that the lower band observed correspond to the light chains of IgM. Western blots done in nonreduced conditions and flow cytometric analysis confirmed that RRCL up-regulate IgM (Fig. 4B and C). Furthermore, the low molecular bands were detected in Western blotting studies where only the secondary antibody (a mouse anti-human horseradish peroxidase–conjugated antibody) was used (data not shown).

Changes of CD20 expression in RRCL occur at both the gene and posttranslational levels. The changes in CD20 expression detected by Western blot may be a result of either alternative splicing or posttranslational (protein) processing. To determine if the resistant lines contained full-length CD20 transcripts, we first isolated cDNA from Raji and the resistant lines 2R and 4RH and amplified the gene using primers to the 5′ (NH_2-terminal) and 3′ (COOH-terminal) ends to determine the sequence. The gene sequences between Raji and RRCL 2R and 4RH are identical, indicating that 2R and 4RH both contain full-length CD20 transcripts (not shown).

To evaluate alternative splicing as a potential mechanism to explain the changes in CD20 expression, we did Northern blot studies and show similar splicing forms between Raji versus 2R and 4RH cells (not shown). Together, these data argue that the resistant lines 2R and 4RH contain full-length CD20 transcripts

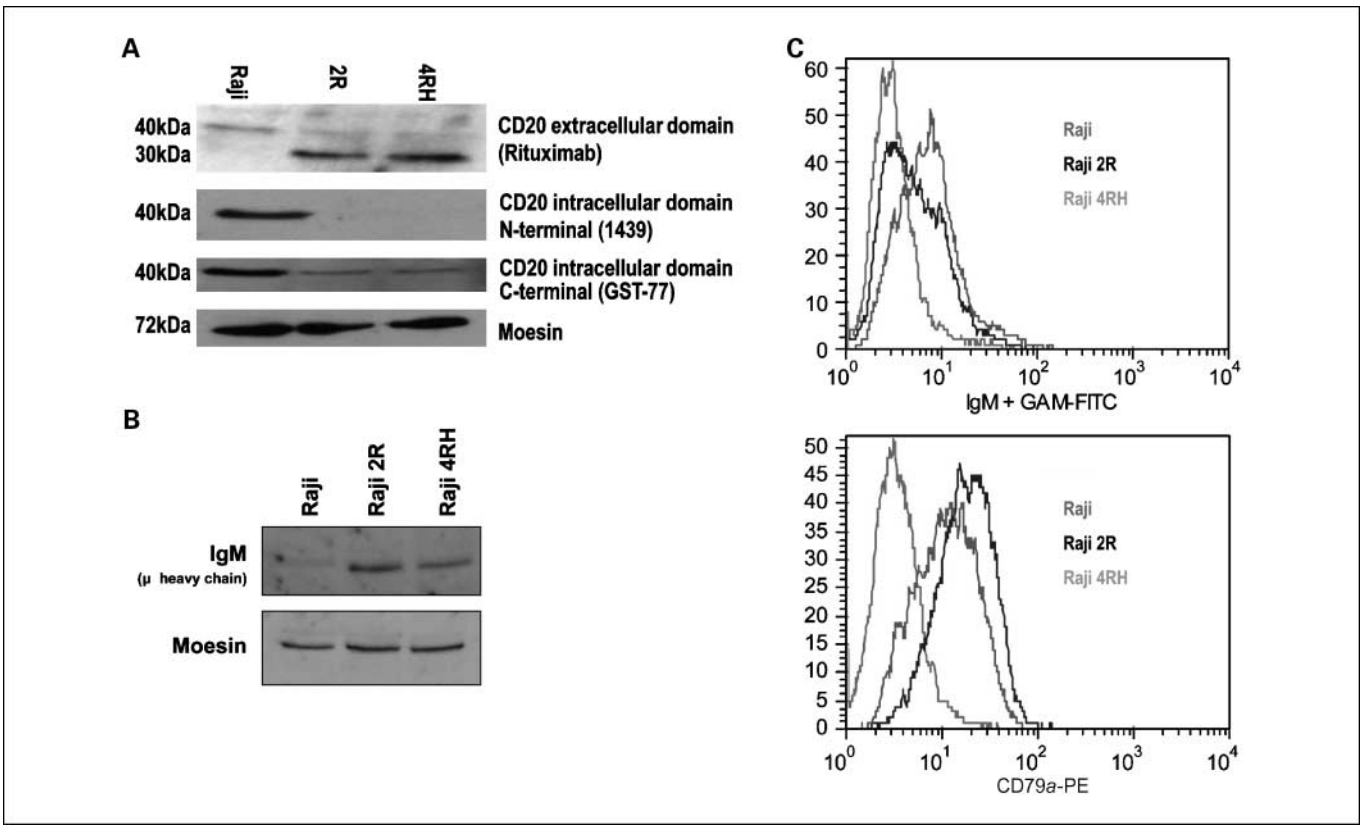

Fig. 4. Up-regulation of IgM in RRCL. Western blotting in reducing conditions revealed a down-regulation of CD20 and a lower molecular weight band in the 34 kDa range (*A*). Subsequent studies have shown that the lower molecular weight band observed corresponded to the IgM light chain. Acquisition of rituximab resistance resulted in up-regulation of IgM and CD79a (*B* and *C*, respectively).

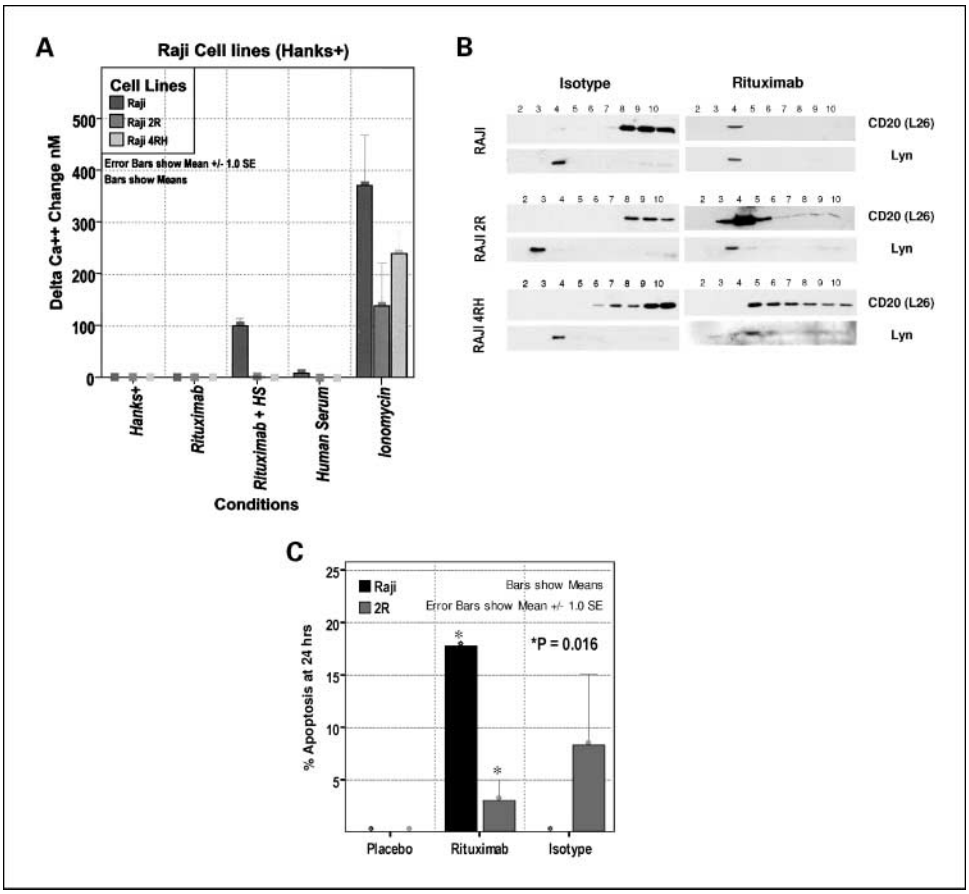

Fig. 5. Differences in signaling events between RSCL and RRCL. *In vitro* exposure to rituximab induces Ca^{2+} mobilization from both the extracellular compartment in Raji cells, but not in RRCL 2R and 4RH (*A*). Extracellular and intracellular Ca^{2+} mobilization was measured by flow cytometric analysis using FLUO-3 AM (acetoxymethyl ester). Pluronic acid F-127 was used to load FLUO-3 AM into NHL cells. Optimization of the Ca^{2+} indicator and calibration curves was done for each cell line. Raji and RRCL were labeled under optimal conditions with FLUO-3 AM/Pluronic Acid F-127. Subsequently, cells were then resuspended in Hanks' medium with Ca^{2+} and exposed to rituximab or isotype (10 mg/mL) ± human serum (25%). Ionomycin was used as a positive control. Isolation of LRD following rituximab exposure shows differences in the redistribution of CD20 antigen into the lipid raft fractions (*lanes 3-5*) between Raji parental cells and RRCL. Lyn is used to colocalize the LRD region. Although there is evidence of redistribution of CD20, it is "incomplete" because a significant amount of CD20 remains in the nonlipid raft fractions (i.e., *lanes 6-10*; *B*). Induction of apoptosis following rituximab (no cross-linking) exposure is significantly decreased in RRCL (Raji 2R) as shown by flow cytometry analysis staining for Annexin V/propidium iodine (*C*).

and that the transcript forms are similar to that observed in Raji cells.

To determine if full-length CD20 protein is synthesized in the resistant lines, we initiated [^{35}S]methionine metabolic labeling studies. Following a 2 h labeling, immunoprecipitation using rituximab was done; Raji 2R cells synthesizes less the full-length CD20 protein than parental Raji, but 2R also shows two faster migrating species (not shown). The faster migrating species may represent shorter versions of CD20 protein processed (within the 2 h labeling time) in addition to the full-length CD20.

Impaired Ca^{2+} mobilization in RRCL is associated with changes in CD20 antigen expression. Various investigators have shown significant mobilization of Ca^{2+} following *in vitro* exposure to rituximab in lymphoma cell lines. It has been postulated that CD20 may directly serve as a calcium channel. Because we found a down-regulation of CD20 in our RRCL, we subsequently investigated if the down-regulation of CD20 could potentially affect downstream signaling events in RRCL. Using real-time flow cytometric detection of FLUO-3 AM fluorescence following exposure of cells to rituximab and human serum revealed a significant decrease in the ability of RRCL to flux calcium in response to rituximab cross-linking (Fig. 5A) compared with parental cells.

Differences in the reorganization of CD20 antigen into LRD and induction of apoptosis upon rituximab binding in RSCL and RRCL. Other groups of investigators have shown that the COOH-terminal region of CD20 antigen is necessary for the reorganization and stabilization of CD20 into the LRD (18). Moreover, disruption of the cholesterol content within the LRD results in a decrease in CD20 recruitment into the LRD region and impairment in rituximab-mediated CMC. Studies using Raji cells and the RRCL 2R and 4RH show that the reorganization of CD20 into the LRD is impaired following rituximab exposure compared with the parental Raji cells (Fig. 5B). In addition, a decrease in rituximab-induced direct apoptosis was observed in RRCL (Fig. 5C).

Gene profile changes associated with the acquisition of resistance to rituximab. To elucidate potential pathways involved in the development of rituximab resistance and possibly CD20 antigen expression, we studied differences in the gene expression profiles between rituximab-sensitive Raji cells with the two RRCL derived from it (i.e., 2R and 4RH). Applying cDNA microarray technology, a total of 11,519 genes were screened. Our studies showed that significant changes in expression of genes occur in rituximab-resistant cells when compared with their rituximab-sensitive parental cells. A total of 148 genes were found to been up-regulated in 2R cells and 365 genes in the 4RH cells when compared with the Raji parental cell lines. In addition, down-regulation of 10 genes (2R cells) and 23 genes (4RH) were detected in rituximab-resistant cells, respectively. Common genetic changes were observed between the 2R and 4RH cell lines. A common subset of 129 up-regulated genes and 10 down-regulated genes were detected in both 2R and 4RH cells (Supplementary Table 1A and B). Of interest, a significant up-regulation of genes from proteins involved in the ubiquitin-proteasome system was noted (Table 2). Confirmatory studies at the protein level showed an

increase in the proteasome activity (Supplementary Fig. 2A-C) and up-regulation of the ubiquitin-conjugating enzymes E1 and E2 in 2R and 4RH cells (Supplementary Fig. 2D).

Effects of proteasome inhibition in CD20 expression and rituximab antitumor activity in RRCL. *In vitro* exposure of RRCL to PS341 (20 and 100 nmol/L) for 24 and 48 h resulted in an increased expression of the COOH-terminal region of the internal domain of CD20 (Fig. 6A). No changes were observed in the expression of the NH_2-terminal region of CD20 or rituximab binding site. In addition, PS341-exposed RRCL regained little to no sensitivity to rituximab-associated CMC (Fig. 6B-D). The minimal improvement in rituximab responsiveness strongly suggests that additional alternative mediators of rituximab resistance exist.

Discussion

Upon selective pressure, it is expected that malignant cells will undergo genetic and phenotypic changes that will allow a particular cell clone to survive and expand in a "hostile" environment.

The structure of CD20 was described initially by Tedder et al. (34). CD20 is a tetra-span transmembrane protein with a cytoplasmic COOH- and NH_2-terminal found in normal and neoplastic B cells. CD20 antigen function has not yet been defined. It has been described as a calcium channel or a receptor necessary for B-cell proliferation/maturation (35, 36). However, CD20 knockout mice develop an entire normal B-cell repertoire and places into question its specific role in B-cell proliferation/maturation. Most of our limited knowledge about CD20 function has been obtained using various anti-CD20 murine or chimeric antibodies (B1, MCF7, rituximab, etc.; ref. 37). Although the gene sequence of CD20 is preserved in our RRCL when compared with their parental cell lines, the rate of *CD20* gene transcription and protein degradation changed upon the acquisition of rituximab resistance. Our cell model of rituximab resistance can potentially improve our understanding of CD20 function in normal and malignant B-cell development. Moreover, we noted a previously undocumented up-regulation of surface and/or cytoplasmic IgM in various RRCL. Although the significance of this up-regulation of IgM in RRCL is unknown, it continues to be part of ongoing research in our laboratory.

The acquisition of resistance to anti-idiotypic mAbs was described previously by Levi et al. (19). "Complete" loss of expression of CD20, the most plausible mechanism to explain rituximab resistance, has been observed only in a relatively small number of patients (20). Our data suggest that chronic exposure to rituximab results in both global gene and protein down-regulation of CD20. Similar to our findings, other groups of investigators had previously shown that the chronic exposure of B-cell lymphoma cell lines to rituximab results in acquirement of rituximab resistance and down-regulation of CD20 (38, 39). Despite differences in the cell lines used or the strategy to develop rituximab resistance in cell lines used by Drs. Bonavida's, Aizawa's, or our group of investigators, the common finding was the global down-regulation of CD20 antigen. Of interest, although it is beyond the scope of this article, the acquirement of rituximab resistance in B-cell lymphoma cell lines is associated with deregulation of the

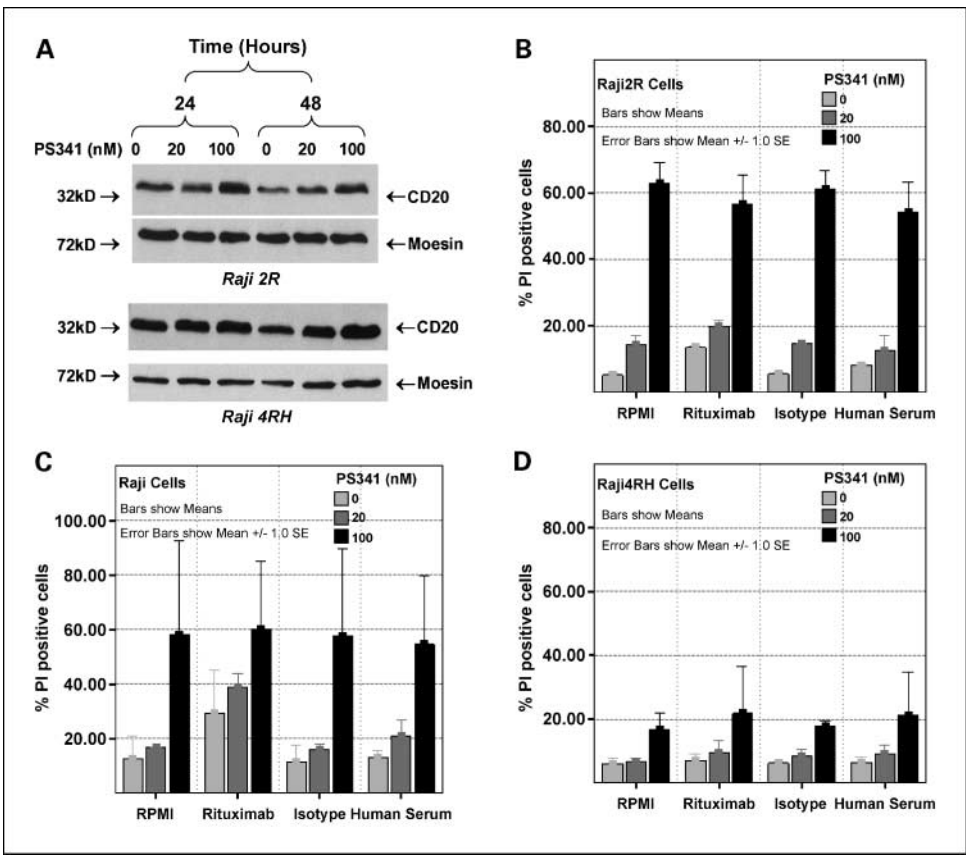

Fig. 6. The role of proteasome-ubiquitin system in rituximab resistance and CD20 expression. *In vitro* exposure of RRCL (Raji 2R and Raji 4RH) to bortezomib (PS341, 20 or 100 nmol/L) resulted in an increase expression of CD20 as shown by Western blotting (a GST-77 recognizing the COOH-terminal region of human CD20 was used; *A*). Despite an increase in CD20 antigen expression following *in vitro* exposure to bortezomib (low doses, i.e., 20 nmol/L), there was little to no changes in rituximab-mediated CMC in RRCL, suggesting the existence of additional mechanisms responsible for rituximab resistance (*B-D*). Briefly, RSCL or RRCL were exposed to either DMSO or bortezomib (PS341) for 48 h and subsequently exposed to RPMI, rituximab, or isotype (10 mg/mL), and 25% human serum for 6 h. Necrosis was detected by propidium iodide (*PI*) staining. Experiments were done in triplicates.

apoptotic machinery leading to resistance to multiple chemotherapy agents as shown by Dr. Bonavida's group, as well as in our rituximab resistance cell models (39, 40).

Compared with other rituximab-resistant cell models, our RRCL are able to maintain low levels of CD20 and resistance to rituximab *in vitro* or *in vivo* (Raji 2R and Raji 4RH cells tested) without the necessity to be maintained in rituximab-containing medium for long periods of time (39).

The regulation of CD20 expression in RRCL is complex and at least involves transcriptional and posttranscriptional regulatory mechanisms. The absence of point mutations in our gene sequencing studies and the formation of two identical alternative splicing isoforms in our Northern blot studies further favor a posttranscriptional event. Our data suggests that the ubiquitin-proteasome system may play a role in the degradation of the COOH-terminal region of CD20 in RRCL. It is unclear how the proteasome regulates CD20 expression in our RRCL, and two hypothesis could be formulated. The first one entertains a direct role of the proteasome in CD20 protein degradation. Investigators have shown that several transmembrane receptors, such as HLA-class II or FcεRI, undergo ubiquitination and proteasome degradation; FcεRI shares structural similarities with CD20 (41–44). The second hypothesis postulates that the proteasome indirectly regulates CD20 expression by targeting a CD20-regulatory transcription factor (45–47). Ongoing studies in our laboratory are focused in addressing the mechanism(s) by which the proteasome regulates CD20 expression in RRCL. To our knowledge, this is the first report suggesting that CD20 expression may be regulated by the ubiquitin-proteasome system. By selectively inhibiting the proteasome, we were able to increase the expression of the COOH-terminal region of CD20 in RRCL. Despite the changes in CD20 expression following *in vitro* exposure to PS341, only partial improvement in rituximab-associated CMC was observed, suggesting the existence of other mechanisms of acquired resistance to rituximab (i.e., up-regulation of CD55 and CD59). In addition, we discovered an unanticipated up-regulation of the CD52 antigen in RRCL. Although the significance of this finding is unclear, it is possible that targeting CD52 with alemtuzumab may result in significant antitumor activity and could potentially be used in the treatment of rituximab-refractory B-cell lymphomas. It is important to acknowledge that our results are primarily limited to our lymphoma model and will need to be validated in cells directly derived from patients with primary rituximab refractory B-cell lymphomas.

Lipid raft domains (LRD) are defined as cholesterol- and sphingolipid-rich microdomains that are resistant to solubilization in nonionic detergents at low temperatures (48). LRD undergo significant structural changes during activation states such as receptor-ligand (e.g., antigen-mAb) binding or chemical exposure (49, 50). The abnormal down-regulation of CD20 antigen, such as that found in our RRCL, although not affecting binding of rituximab, affected the redistribution of CD20 antigen into LRDs. Down-regulation of CD20 potentially results in a decrease in signaling events as shown in our Ca^{2+} influx studies. Ongoing studies are aimed to further study the changes in calcium mobilization, Ca^{2+} storage, and regulatory proteins, and the differences in tyrosine phosphorylation between RSCL and RRCL. In addition, validation of our findings in a more clinically relevant "model" such as from "paired" primary B-cell lymphoma patient samples is needed and is under way under institutional review board approval protocols. As more lymphoma patients are exposed to prolonged rituximab maintenance programs, the potential risk of acquired "biological" resistance will likely increase. In anticipation of this clinical scenario, it is necessary to define the mechanisms of resistance to rituximab so that rational strategies to overcome it may be designed, tested, and clinically implemented. Our model is a valuable tool by which to define mechanisms/pathways associated with rituximab resistance.

References

1. Chu PG, Loera S, Huang Q, Weiss LM. Lineage determination of CD20- B-cell neoplasms: an immunohistochemical study. Am J Clin Pathol 2006;126:534–44.
2. Deans JP, Schieven GL, Shu GL, et al. Association of tyrosine and serine kinases with B cell surface antigen CD20. J Immunol 1993;151:4494–504.
3. Shan D, Ledbetter JA, Press OW. Apoptosis of malignant human B cell by ligation of CD20 with monoclonal antibodies. Blood 1998;91:1644–52.
4. Shan D, Ledbetter JA, Press OW. Signaling events involved in anti-CD20-induced apoptosis of malignant human B-cells. Cancer Immunol Immunother 2000;48:673–83.
5. Popoff IJ, Savage JA, Blake J, Johnson P, Deans JP. The association between CD20 and Src-family tyrosine kinases requires an additional factor. Mol Immunol 1998;35:207–14.
6. Taji H, Kagami Y, Okada Y, et al. 1998. Growth inhibition of CD20-positive B lymphoma cell lines by IDEC-C2B8 anti-CD20 monoclonal antibody. Jpn J Cancer Res 1998;89:748–56.
7. Holder M, Grafton G, MacDonald I, Finney M, Gordon J. Engagement of CD20 suppress apoptosis in germinal center B cells. Eur J Immunol 1995;25:3160–4.
8. Mathas S, Rickers A, Bommert K, Dorken B, Mapara MY. Anti-CD20 and B-cell receptor-mediated apoptosis: evidence for shared intracellular signaling pathways. Cancer Res 2000;60:7170–6.
9. Hofmeister JK, Cooney D, Coggeshall KM. Clustered CD20 induced apoptosis: Src-family kinase, the proximal regulator of tyrosine phosphorylation, calcium influx, and caspase 3-dependent apoptosis. Blood Cells Mol Dis 2000;26:133–43.
10. Harjunpaa A, Junnikkala S, Meri S. Rituximab (anti-CD20) therapy of B-cell lymphomas: direct complement killing is superior to cellular effector mechanisms. Scand J Immunol 2000;51:634–41.
11. Cragg MS, French RR, Glennie MJ. Signaling antibodies in cancer therapy. Curr Opin Immunol 1999;11:541–7.
12. Hernandez-Ilizaliturri FJ, Jupudy V, Oflazoglu E, et al. Neutrophils contribute to the biological anti-tumor activity of rituximab in a non-Hodgkin's lymphoma severe combined immunodeficiency (SCID) mouse model. Clin Cancer Res 2003;9:5866–73.
13. Clynes RA, Towers TL, Presta LG, Ravetch JV. Inhibitory Fc receptors modulate *in vivo* cytotoxicity against tumor targets. Nat Med 2000;4:443–6.
14. Semac I, Palomba C, Kulangara K, et al. Anti-CD20 therapeutic antibody rituximab modifies the functional organization of rafts/microdomains of B lymphoma cells. Cancer Res 2003;63:534–40.
15. Polyak M, Tailor SH, Deans JP. Identification of a cytoplasmic region of CD20 required for its distribution to a detergent-insoluble membrane compartment. J Immunol 1998;161:3242–8.
16. Davis TA, Grillo-Lopez AJ, White CA, et al. Rituximab anti-CD20 monoclonal antibody therapy in non-Hodgkin's lymphoma: safety and efficacy of retreatment. J Clin Oncol 2000;18:3135–43.
17. Czuczman MS, Grillo-Lopez AJ, White CA, et al. The treatment of patients with low-grade b-cell lymphoma with the combination of chimeric anti-CD20 monoclonal antibody (Rituxan, rituximab) and CHOP chemotherapy. J Clin Oncol 1999;17:268–76.
18. Coiffier B, Lepage E, Briere J, et al. CHOP Chemotherapy plus rituximab compared with CHOP alone in elderly patients with diffuse large-B-cell lymphoma. et al. N Engl J Med 2002;346:235–242.
19. Meeker T, Lowder J, Cleary ML, et al. Emergence of idiotype variants during treatment of B-cell lymphomas with anti-idiotype antibodies. N Engl J Med 1985;312:1658–5.
20. Davis T, Czerwinski DK, Levy R. Therapy of B-cell lymphoma with anti-CD20 antibodies can results in the loss of CD20 antigen expression. Clin Cancer Res 1999;5:611–5.
21. Cartron G, Dacheux L, Salles G, et al. Therapeutic activity of humanized anti-CD20 monoclonal antibodies and polymorphism in IgG Fc receptor FcγRIIIa gene. Blood 2002;99:754–8.
22. Golay J, Zaffaroni T, Lazzari M, et al. Biological

response of B-lymphoma cells to anti-CD20 monoclonal antibody rituximab *in vitro*: CD55 and CD59 regulate complement-mediated lysis. Blood 2000; 95:3900–8.

23. Simpson KL, Norman JA, Holmes CH. Expression of complement regulatory proteins decay accelerating factor (DAF, CD55), membrane cofactor protein (MCP, CD46) and CD59 in the normal human uterine cervix and in premalignant cervical disease. Am J Pathol 1997;151:1455–67.

24. Niehans GA, Cherwitz DL, Staley NA, Knapp DJ, Dalmasso AP. Human carcinomas variably express the complement inhibitory proteins CD46 (membrane cofactor protein), CD55 (decay-accelerating factor), and CD59 (protectin). Am J Pathol 1996; 149:129–42.

25. Lehmann C, Zeis M, Schmitz N, Uharek L. Impaired binding of perforin on the surface of tumor cells is a cause of target cell resistance against cytotoxic effector cells. Blood 2000;96:594–600.

26. Treon SP, Mollick JA, Urashima M, et al. Muc-1 core protein is expressed on multiple myeloma cells and is induced by dexamethasone. Blood 1999;93: 287–1298.

27. Polyak MJ, Ayer LM, Szczepek AJ, Deans JP. A cholesterol-dependent CD20 epitope detected by the FMC7 antibody. Leukemia 2003;17:1384–9.

28. Otonello L, Marone P, Dapino P, Dallegri F. Monoclonal Lym-1 antibody-dependent lysis of B-lymphoblastoid tumor targets by human complement and cytokine exposed mononuclear and neutrophilic polymorphonuclear leukocytes. Blood 1996;87:5171.

29. Chomczynski P, Mackey K. Substitution of chloroform by bromo-chloropropane in the single step method of RNA isolation. Anal Biochem 1995;225: 163–4.

30. Wilkinson M. Purification of RNA. In: Brown TJ, editor. Essential molecular biology: a practical approach, vol. 1. Oxford: Oxford University Press; 1991; p. 69–87.

31. Alwine JC, Kemp DJ, Stark GR. Method for detection of specific RNAs in agarose gels by transfer to diazobenzyloxymethyl-paper and hybridization with DNA probes. Proc Natl Acad Sci U S A 1977;74: 5350–4.

32. Askew D, Chu RS, Krieg AM, Harding CV. CpG DNA induces maturation of dendritic cells with distinct effects on nascent and recycling MHC-II antigen-processing mechanisms. J Immunol 2000;165:6889.

33. Cheng PC, Dykstra ML, Mitchell RN, Pierce SK. A role for lipid rafts in B cell antigen receptor signaling and antigen targeting. J Exp Med 1999;6:1549–60.

34. Tedder TF, Streuli M, Schlossman SF, Saito H. Isolation and structure of a cDNA encoding the B1 (CD20) cell-surface antigen of human B lymphocytes. Proc Natl Acad Sci U S A 1988;85:208–12.

35. Deans JP, Kalt L, Ledbetter JA, Schieven GL, Bolen JB, Johnson P. Association of 75/80-kDa phosphoproteins and the tyrosine kinases Lyn, Fyn, and Lck with the B cell molecule CD20. Evidence against involvement of the cytoplasmic regions of CD20. J Biol Chem 1995;270:22632–8.

36. Pedersen IM, Buhl AM, Klausen P, Geisler CH, Jurlander J. The chimeric anti-CD20 antibody rituximab induces apoptosis in B-cell chronic lymphocytic leukemia cells through a p38 mitogen activated protein-kinase-dependent mechanism. Blood 2002;99: 1314–9.

37. Alas S, Emmanouilides C, Bonavida B. Inhibition of interleukin 10 by rituximab results in down-regulation of Bcl-2 and sensitization of B-cell non-Hodgkin's lymphoma to apoptosis. Clin Cancer Res 2001;7: 709–23.

38. Jazirehi AR, Vega MI, Bonavida B. Development of rituximab-resistant lymphoma clones with altered cell signaling and cross-resistance to chemotherapy. Cancer Res 2007;67:1270–81.

39. Takei K, Yamazaki T, Sawada U, Ishizuka H, Aizawa S. Analysis of changes in CD20, CD55, and CD59 expression on established rituximab-resistant B-lymphoma cell lines. Leuk Res 2006;30:625–31.

40. Olejniczak SH, Hernandez-Ilizaliturri FJ, Clements JL, Czuczman MS. Loss of expression of the pro-apoptotic Bcl-2 family proteins Bak and Bax in rituximab- and chemotherapy-resistant non-Hodgkin's lymphoma cells [abstract presented during the 2005 ASH meeting]. Blood 2005;106:4819.

41. Ciechanover A. The ubiquitin-proteasome proteolytic pathway. Cell 1994;79:13–21.

42. Hochstrasser M. Ubiquitin, proteasomes and the regulation of intracellular protein degradation. Curr Opin Cell Biol 1995;7:215–23.

43. Qu X, Sada K, Kyo S, Maeno K, Miah SM, Yamamura H. Negative regulation of FcεRI-mediated mast cell activation by a ubiquitin-protein ligase Cbl-b. Blood 2004;103:1779–86.

44. Gingras MC, Lapillonne H, Margolin JF. CFFM4: a new member of the CD20/FcεRIβ family. Immunogenetics 2001;53:468–76.

45. Ciechanover A. The ubiquitin-proteasome pathway: on protein death and cell life. EMBO J 1998; 17:7151–60.

46. Spataro V, Norbury C, Harris AL. The ubiquitin-proteasome pathway in cancer. Br J Cancer 1998;77: 448–55.

47. Pahl HL, Baeuerle PA. Control of gene expression by proteolysis. Curr Opin Cell Biol 1996;8:340–7.

48. Simons K, Ikonen E. Functional rafts in cell membranes. Nature 1997;387:569–72.

49. Wang X-Y, Ostberg JR, Repasky EA. Effect of fever-like whole body hyperthermia on lymphocyte spectrin distribution, protein kinase C activity and uropod formation. J Immunol 1999;162:3378–87.

50. Janes PW, Ley SC, Magee AI, Kabouridis PS. The role of lipid rafts in T cell antigen receptor signalling. Semin Immunol 2000;12:23–34.

Clinical Cancer Research

Acquirement of Rituximab Resistance in Lymphoma Cell Lines Is Associated with Both Global *CD20* Gene and Protein Down-Regulation Regulated at the Pretranscriptional and Posttranscriptional Levels

Myron S. Czuczman, Scott Olejniczak, Aruna Gowda, et al.

Clin Cancer Res 2008;14:1561-1570.